Hindawi
Geofluids
Volume 2021, Article ID 5549223, 11 pages
https://doi.org/10.1155/2021/5549223

Research Article

A Study of Instantaneous Shear Mechanical Properties on the Discontinuity of Rock Mass Based on 3D Morphological Properties

Qingzhao Zhang,[1,2] Zejun Luo,[1,2] Bo-An Jang,[3] Qiuyi Wang,[4] Zhen Zhong,[5] and He Jiang[6]

[1]*Department of Geotechnical Engineering, Tongji University, Shanghai, China*
[2]*Key Laboratory of Geotechnical and Underground Engineering of Ministry of Education, Tongji University, Shanghai, China*
[3]*Department of Geophysics, Kangwon National University, 1Kangwondaehak-gil, Chuncheon-si, Gangwon-do 24341, Republic of Korea*
[4]*Yunnan Gongdong Expressway Construction Headquarters, Kunming, China*
[5]*Key Laboratory of Rock Mechanics and Geological Hazards of Zhejiang Province, Shaoxing University, Zhejiang Province, China*
[6]*YCIC Highway Construction Co., Ltd, Kunming, China*

Correspondence should be addressed to Zhen Zhong; zhongzhen@zju.edu.cn

Received 13 February 2021; Revised 2 November 2021; Accepted 11 November 2021; Published 28 November 2021

Academic Editor: Kai Yao

In order to study the instantaneous mechanical properties of rock mass discontinuities with different 3D morphologies during the shear process, the Brazilian splitting method is used to prepare natural rock mass discontinuities, and the high-precision 3D scanning test of discontinuities is carried out. The Z_2 is selected as the evaluation parameter of the discontinuities. Based on the graded cyclic shear test results of discontinuities, the influence of the morphology characteristics on the strength and deformation characteristics is analyzed. With the increase of shear times, the 3D morphology characteristic parameters of the structural plane decrease steadily after the graded cyclic shear. Based on the test curve, the graded cyclic shear characteristics of rock mass discontinuities are analyzed from the shear deformation, and the shear process of the discontinuities is finely divided by combining with the variation characteristics of shear stiffness. Combined with the 3D morphology parameters, an empirical formula for the shear strength of discontinuities is proposed. Through verification, the effect of the new model is better than that of the classical JRC-JCS model.

1. Introduction

The discontinuities in jointed rock mass play a dominant role in the deformation and damage of rock mass. Due to the existence of discontinuities, the rock mass has complex engineering properties, which leads to anisotropy and heterogeneity [1]. Meanwhile, it also destroys the integrity of the rock mass and greatly reduces the material properties of the rock mass, which is the primary factor that affects the stability of engineering rock mass [2]. Therefore, scholars have always been focusing on the study on the mechanical properties and parameter selection of the discontinuities of rock mass.

The morphological properties of the discontinuities of rock mass have a significant impact on their mechanical properties [3, 4]. Speaking of two-dimensional morphological properties of discontinuities, the most famous of which is the joint morphology characterized by joint roughness coefficient (JRC) of the discontinuities proposed by Barton and Choubey [5]. The method has now been recommended by the International Society for Rock Mechanics and Engineering. In fact, many scholars have modified and improved the

JRC evaluation method and also established a quantitative empirical relationship between different statistical parameters and JRC values by measurement and statistical methods [6–9]. Since Prof. Mandelbrot proposed the theory of fractal geometry [10], some scholars have applied it to the study of jointed morphology. Kulatilake et al. and Zhu et al. [11, 12] separately established an empirical relationship between fractal dimensions and JRC indicators, so that JRC indicators can be obtained by a fractal method. In recent years, the characterization method for the 3D morphology of discontinuities has become a hot topic in the research of morphological characteristics. Belem et al. [13] discussed the 3D roughness coefficient characterizing the morphology of several discontinuities and studied the variation law of the roughness coefficient in the shear process of discontinuities. Grasselli et al. [14] studied the morphological properties of discontinuities with 3D morphology scanning technology, proposing to describe the 3D morphological properties of discontinuities with new 3D morphological parameters. Xia et al. [15] studied the description of the 3D morphology of discontinuities in different contact states and proposed the method of calculating morphological parameters. Rabczuk et al. [16, 17] described a new approach for modelling discrete cracks in mesh-free methods. At present, the study on the morphological properties of discontinuities and their characterization methods has been mature, but it still needs to be further improved. The characterization methods of 3D morphology of discontinuities have higher requirements for measurement accuracy, and the characterization parameters are complex, which are not conducive to popularization and promotion.

Shear strength is one of the basic mechanical properties of discontinuities, and rich research results have now been achieved. Among the studies on the strength properties of discontinuities, the most representative of which is three strength formulas of discontinuities, i.e., Patton's formula, Ladanyi's formula, and Barton's formula, and most of the follow-up studies are carried out based on these three formulas. Patton introduced undulating angle into Mohr-Coulomb criterion in the 1960s and established the bilinear shear strength criterion of discontinuities. Barton [18] established the famous empirical formula of JRC-JCS peak shear strength based on JRC indicators. Chen et al. [19] constructed the model of peak shear strength based on the function relationship between normal stress and peak-dilation angle of discontinuities. Park et al. [20] constructed a shear constitutive model of discontinuities based on 3D morphological parameters. Based on the study of the 3D morphology of discontinuities. Xia et al. [21] carried out a comprehensive study on the 3D peak shear strength of discontinuities and constructed a 3D model of peak shear strength. Ge [22] established the empirical formula for the peak shear strength of discontinuities based on the 3D morphological parameter BAP. Compared with the strength properties of the discontinuities of rock mass, the study on its deformation properties is inferior in both depth and breadth, but the scholars at home and abroad have never stopped studying the deformation properties of discontinuities [23, 24]. Yin et al. [25] constructed a new discontinuities constitutive model based on cyclic shear test and numerical simulation and reflected the impact of the wear of discontinuities on its frictional characteristics and dilation characteristics in the model. Li and Du [26] explored the shear deformation characteristics of discontinuities based on the shear test on artificial discontinuities. Huang et al. [27] simulated the shear test on the regularly dentate discontinuities with different normal stresses and angles based on PFC2D program and analyzed the law of shear deformation and strength. Gui [28] established the jointed peak shear displacement model based on the direct shear test on artificial discontinuities and proposed the constitutive model of joint shear and the shear dilatancy mode. The research results of the mechanical properties of discontinuities are mainly in the artificially prefabricated regular discontinuities, while there are relatively less studies on the natural rock mass discontinuities. In particular, there are few studies considering the 3D morphological properties of rock mass discontinuities.

The morphological properties of discontinuities are fundamental for studying the strength theory, but it is difficult to apply the current strength model due to the complex characterization method of 3D morphological properties of discontinuities. In this paper, several samples of discontinuities of natural rock mass are prepared through artificial fracturing with the help of 3D morphology scanning technology, and the 3D morphological properties are evaluated. The graded cyclic shear test of discontinuities is carried out based on different 3D morphological properties, and the impact of which on the strength of discontinuities is analyzed based on the test results. From the angle of changes in shear strength, the deformation properties of discontinuities in the shear process are studied, and the empirical formula of shear strength of discontinuities considering 3D morphological properties is established.

2. Materials and Methods

2.1. Sample Preparation. Ten natural gneiss blocks are selected to prepare $100 \times 100 \times 100$ mm ($L \times W \times H$) cube samples, and the 100×100 mm ($L \times W$) discontinuities of rock mass are obtained by the Brazil split test in the direction parallel to that of the gneiss schistosity, and the samples of discontinuities are numbered from p-i, as shown in Figure 1.

2.2. Scanning Test on 3D Morphology of Discontinuities. In order to quantitatively characterize the impact of 3D morphology of the discontinuities on the shear strength, as shown in Figure 2, TJXW-3D rock surface morphometry is used to determine the surface morphology of the discontinuities of rock mass. Ten samples of discontinuities in total are selected for graded cyclic shear test. After each direct shear test, the samples shall be provided with 3D morphological scanning for 10 s, with a scanning accuracy of $\pm 20\,\mu$m, so as to accurately obtain 3D morphological data of the discontinuities, as shown in Figure 3.

2.3. Graded Cyclic Direct Shear Test. The CSS-1950 biaxial rheological rock tester in the Key Laboratory of Geotechnical and Underground Engineering, as shown in Figure 4, is used

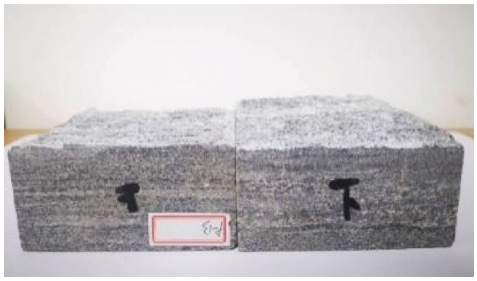

Figure 1: Gneiss discontinuities.

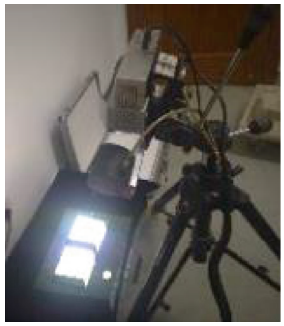

Figure 2: Surface morphometer.

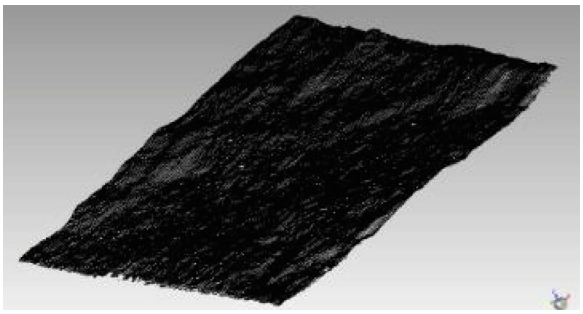

Figure 3: 3D morphological data of discontinuities.

Figure 4: CSS-1950 biaxial rheological rock tester.

to carry out the graded cyclic shear test on the discontinuities of rock mass. The maximum pressure of the tester is 500 kN in the direction of vertical axis and 300 kN in the horizontal direction, and the control accuracy of the loading system is 1%.

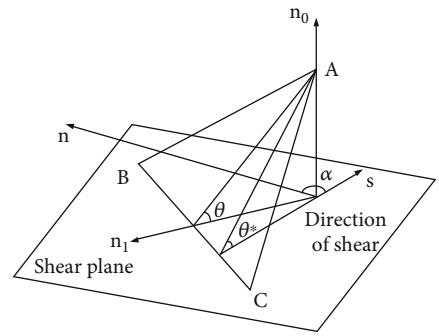

Figure 5: Geometrical relationship diagram of jointed elementary apparent dip algorithm.

The normal load of rock mass shear test shall be determined by the uniaxial compressive strength of rock mass samples. The average uniaxial compressive strength obtained by the uniaxial ultimate compressive strength test on 5 cylindrical samples is 50.5 MPa.

As the anisotropy of discontinuities is complex, the sample blocks are tested by loading the graded cyclic shear under different normal stresses. 5 sample blocks of the discontinuities of natural rock mass are selected. Each sample block of discontinuities is subject to five direct shear tests, respectively (under the normal stresses of 2.5 MPa, 3.75 MPa, 5 MPa, 6.25 MPa, and 7.5 MPa), and the shear rate is 0.5 MPa/min, so that the c and φ values and the morphological changes of each discontinuities are obtained in combination with the test results.

3. 3D Morphological Evaluation of the Discontinuities of Rock Mass

3.1. 3D Morphological Indicators of Discontinuities. Based on a number of shear tests on the discontinuities of rock mass, it is found that there is only partial contact between the top and bottom of rock discontinuities in the shear process, and such contact only appears on the slope facing the shear direction. When determining the 3D morphological properties of discontinuities, parameters facing the shear direction shall be used to reflect the effective shear resistance of the discontinuities. Grasselli et al. studied the morphological properties of discontinuities by means of 3D morphological scanning and pointed out the geometrical relationship between the triangular elementary apparent dip of discontinuities (θ^*) and the shear direction with reference to the concept of effective shear angle (i.e., apparent dip θ^*) [14], as shown in Figure 5.

As shown in Figure 6, the formula of calculating the apparent dip (θ^*) is as follows:

$$\theta^* = \tan^{-1}(-\tan\theta \times \cos\alpha), \tag{1}$$

$$\cos\theta = \frac{\boldsymbol{n} \times \boldsymbol{n_0}}{|\boldsymbol{n}| \times |\boldsymbol{n_0}|}, \tag{2}$$

$$\cos\alpha = \frac{\boldsymbol{s} \times \boldsymbol{n_1}}{|\boldsymbol{s}| \times |\boldsymbol{n_1}|}, \tag{3}$$

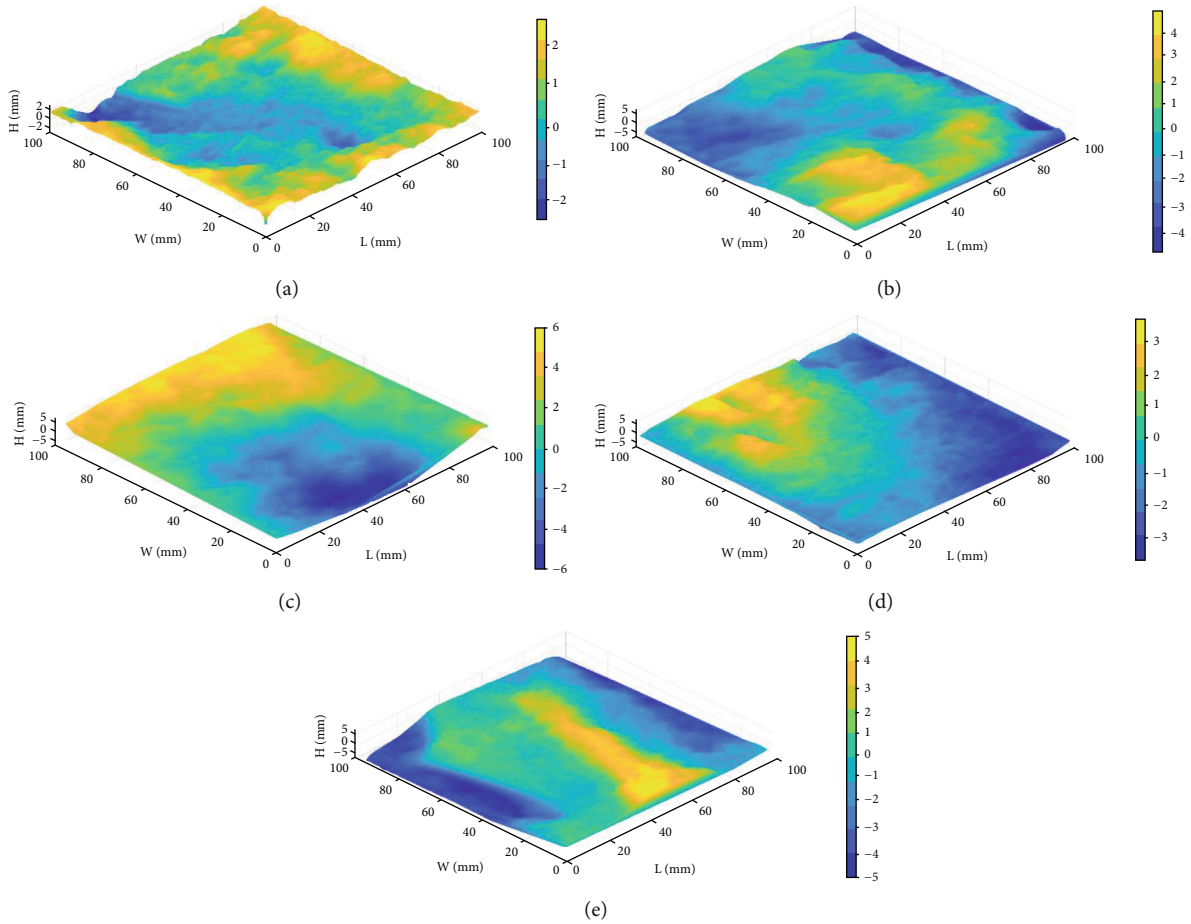

Figure 6: Initial 3D Morphology of Discontinuities. (a) p-1. (b) p-2. (c) p-3. (d) p-4. (e) p-5.

where θ refers to the true dip of triangular element of the discontinuities, α refers to the included angle of triangular element of the discontinuities in dip direction and shear direction, n refers to the outer normal vector of joint element, n_0 refers to the outer normal vector of shear plane, n_1 refers to the projected vector of n in shear direction, and s refers to the vector of joint in shear direction.

Tse and Cruden [29] obtained a logarithmic regression relationship between JRC and Z_2 of joint curve from 10 Barton standard contour curves, which was the most widely used. Yu and Vayssade [30] used a linear relationship to describe the relationship between JRC and Z_2. In 2010, Tatone and Grasselli [31] also proposed to use the exponential relation to represent the relationship between JRC and Z_2. The above research results show that Z_2 can better describe the undulation characteristics of joint.

The relief data after Delaunay in the previous section is calculated according to formula (1), so as to obtain the effective shear dip (θ^*) of each triangular elementary plane.

In this study, according to the effective shear dip (θ^*) calculated of each triangular elementary plane, the formula of calculating the root-mean-square (Z_2) of slope is put forward as follows:

$$Z_2 = \sqrt{\frac{\sum_{i=1}^{n}(\tan^2\theta_i^*)}{n}}, \tag{4}$$

where θ_i^* refers to the effective shear dip of any triangular element and n refers to the number of effective shear dips on the whole joint surface.

Formula (4) is related to the effective shear dip of discontinuities only. The root-mean-square (Z_2) of relief slope finally determined can be used to accurately describe the morphological properties of the whole discontinuities, and the calculation is fast, so that it can be used as a valid parameter for describing the morphological properties of discontinuities.

3.2. Calculation of 3D Morphological Property Indicators of Discontinuities. The point cloud data obtained by scanning the morphology of discontinuities is a coordinate system based on the morphometry projection center, and the samples are placed at will during scanning, so the coordinates shall be transformed before calculating the morphological parameters in order to get the triangular metadata under the standardized coordinate system. Later, the MATLAB program is used to transform the coordinates for the triangular point cloud data, so as to get the triangular elementary data of discontinuities under the global coordinate system, as shown in Figure 6. Also, formula (4) is used to calculate the root-mean-square (Z_2) of slope, a 3D morphological parameter of discontinuities. In this paper, the Z_2 of discontinuities is used to characterize the 3D morphological properties of discontinuities, and the results are shown in Table 1.

Table 1: Root-mean-square values of discontinuities.

Sample No.	Initial	First shear	Second shear	Third shear	Fourth shear	Fifth shear
p-1	0.252	0.262	0.225	0.220	0.215	0.211
p-2	0.280	0.290	0.278	0.275	0.262	0.260
p-3	0.273	0.257	0.234	0.238	0.201	0.198
p-4	0.238	0.234	0.224	0.214	0.208	0.205
p-5	0.279	0.266	0.240	0.233	0.223	0.213

According to the changes in 3D morphological property parameters obtained, as shown in Figure 7, the morphological properties and variation trend of discontinuities can be evaluated, so as to better analyze the variation characteristics of discontinuities in the shear test. The curve in Figure 7 shows a steady decreasing trend, indicating that graded cyclic direct shear conditions, slight cutting, and slip occur to the discontinuities, which slowly reduces the roughness of the discontinuities. However, some data in the curve fluctuate, indicating that obvious shear phenomenon may have occurred during the shear process, which significantly changed the shape of the discontinuities, leading to sudden increase or decrease of Z_2. Finally, the three-dimensional morphology parameters of the discontinuities show a decreasing trend, which reflects that the morphology of the discontinuities tends to be smooth and stable in the multistage shear process.

4. Study of Shear Deformation Properties of Different 3D Morphological Discontinuities

4.1. Shear Deformation Properties of Different 3D Morphological Discontinuities. As discontinuities are complex, the deformation properties are determined by the characteristics of the surface morphology and materials, and Ladanyi and Archambault [32] divided the shear deformation of discontinuities into two parts, i.e., cut deformation and frictional deformation. In the discontinuities with same 3D morphological properties, the greater the normal stress is, the higher the peak strength is, and the more obvious the peak is.

As shown in Figure 8 (p-i-zj-l), due to the effect of stress concentration, when the shear stress exceeds the maximum stress that "convex" can bear, it will cause wear and damage to the surface of discontinuities. When the "convex" is cut off largely, the shear stress will be released largely with an obvious stress drop. Later, the discontinuities will start to have yield failure and generate a large relative displacement to enter the stage of macroslip, and the shear stress is largely provided by frictional force.

As shown in Figure 8 (p-i-zj-2~5), the morphological properties of stress-displacement curve (MPa mm) have significantly changed as compared with first shear. The curve shows a period of significant linear increase in early loading but is missing in the original peak stage and goes directly into the yield stage, so that the shear stress has no obvious change with the increase of shear displacement. It is because the obvious "convex" on the surface of discontinuities has

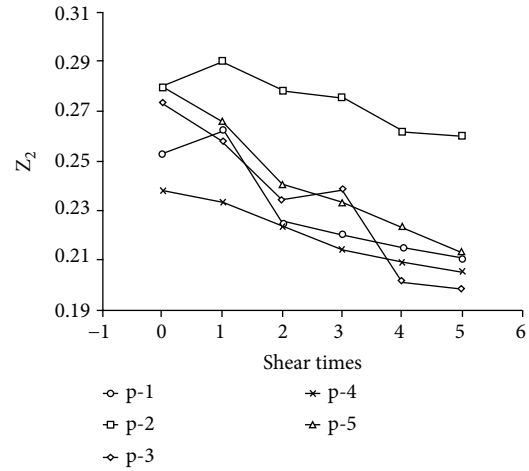

Figure 7: Root-mean-square values of discontinuities.

been cut off during first shear, the discontinuities tend to show "smooth" relief. As the number of shears increases, the whole discontinuities become smoother, the cut phenomenon gradually disappears, and the shear force of the discontinuities is mainly provided by frictional force. Therefore, after the first shear, it is difficult to observe any stress drop in the stress-strain curve as the number of shears increases, and the curve tends to be smoother, which also proves that only the existence of "convex" on the surface of discontinuities makes the discontinuities have a peak during first shear.

4.2. Shear Stiffness Properties of Discontinuities in the Shear Process. From the changes in the shear stiffness of discontinuities in the shear process, the shear process of discontinuities can be described in detail. According to formula (5), the shear stiffness of the discontinuities in the shear process can be calculated. The sample p-1 is used to draw the stress-stiffness-deformation curve, as shown in Figure 9.

$$ks = \frac{\Delta\tau}{\Delta D}. \tag{5}$$

In Figure 9, the shear stiffness shows certain fluctuations. Shear stiffness increases as shear deformation increases at the very beginning, and this stage corresponds to the compaction section (OA section) in the shear curve. Afterwards, shear stiffness sharply increases with deformation, and this stage corresponds to AB section in the shear curve; when shear stress reaches the stress τ_B, the shear stiffness hits the peak, and it later starts to drop, and this stage corresponds to BC section in the shear curve, that is, the sample starts to soften after hardening to the greatest extent; AC section tends to be approximately linear, and this stage is what we called the phase of linear elasticity.

When shear stiffness drops to a certain extent, the shear deformation curve tends to have obvious yield characteristics. At this time, the shear stiffness of discontinuities drops rapidly, and this stage corresponds to CD section in the shear curve, which is the yield stage, as shown in the shear stiffness curve after point N given in Figure 9. When the shear deformation hits the peak, the deformation value

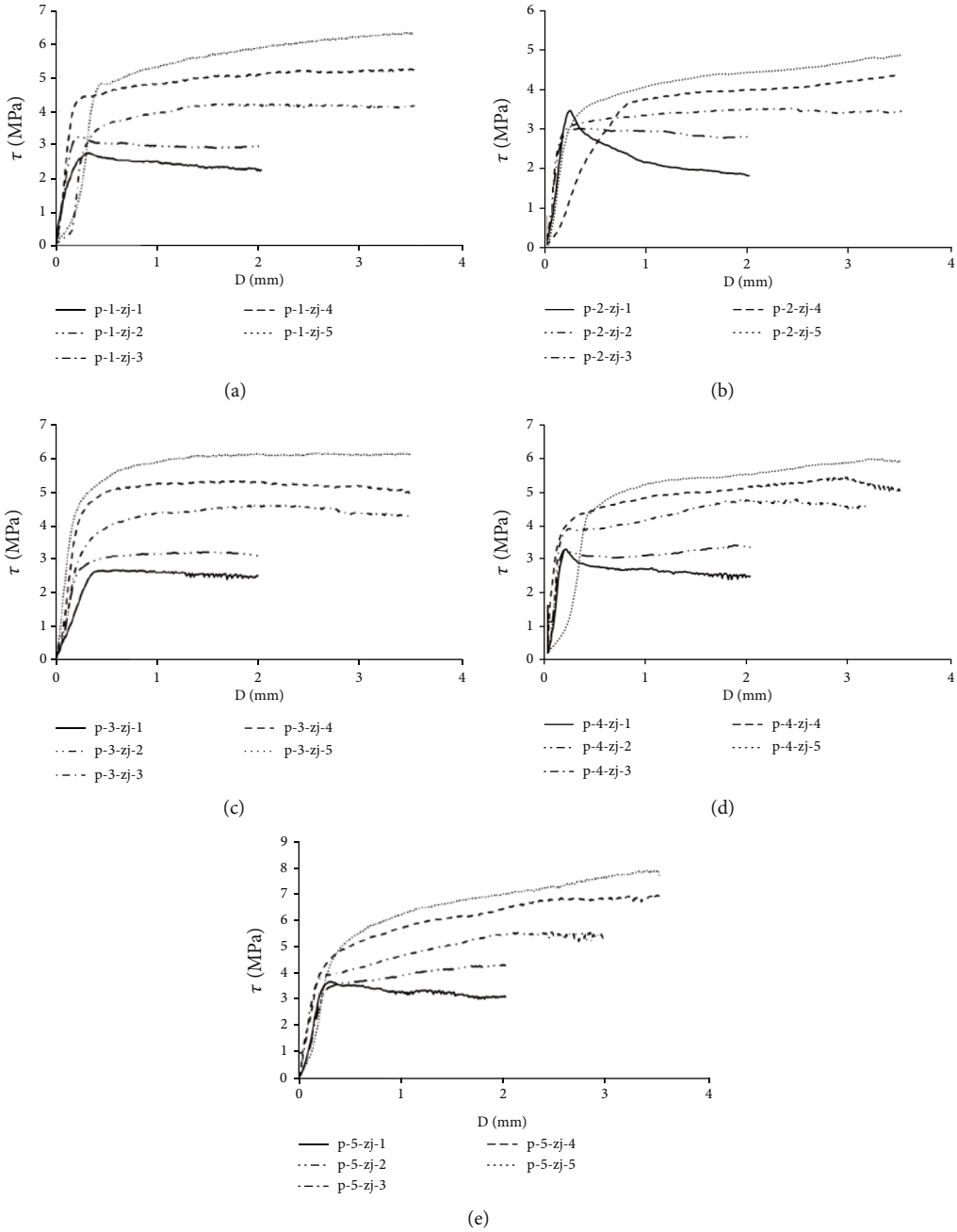

Figure 8: Direct shear stress-displacement curve (MPa mm) of discontinuities with 3D morphological properties under different normal forces. (a) p-1. (b) p-2. (c) p-3. (d) p-4. (e) p-5.

corresponding to point D, the shear stress is maximum, while the shear stiffness is close to zero. When the stress exceeds point D, the shear deformation curve starts to drop, the shear stiffness is negative, and this stage corresponds to the postpeaking phase (DE section), during which the shear stiffness also becomes close to zero from negative.

5. Study of Shear Strength Properties of Different 3D Morphological Discontinuities

5.1. Characteristics of Shear Strength Changes in Discontinuities. As this group of tests is cyclic shear tests on the same sample of discontinuities under different normal pressures, the data processing method may be different. Based on a number of direct shear tests on samples of artificial JRC discontinuities, Wang et al. [33, 34] proposed that the shear strength of discontinuities can be divided into two parts, i.e., the strength component related to the cut and friction.

$$\tau = S_{JRC} + S_f. \tag{6}$$

As it can be seen from formula (6), in the shear process, the shear strength of discontinuities can be divided

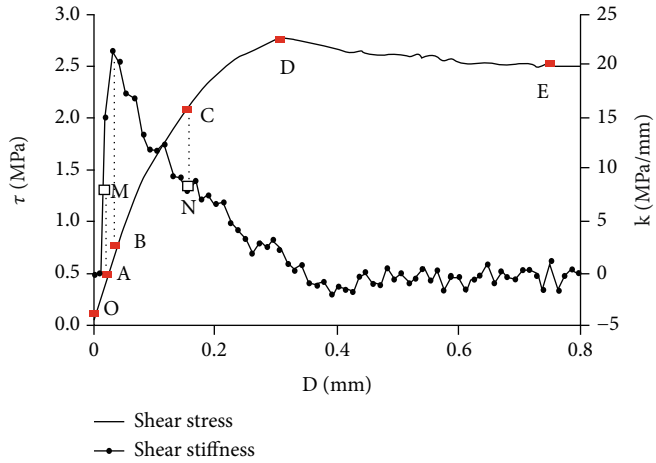

Figure 9: Shear stress-shear stiffness-shear deformation curve.

into two parts, i.e., cut related to JRC and friction between discontinuities. Therefore, it is considered in this paper that this is also the case with the discontinuities of natural rock mass, so that the peak shear strength of discontinuities of natural rock mass can be deemed as being composed of cut and friction approximately.

Figure 10 gives the diagram of strength components of discontinuities of natural rock mass in the shear process. In order to restore the impact of the cut of discontinuities, the peak strength of first shear is subtracted by the residual strength to get the shear stress generated by the cut of discontinuities, which shall later be added to the corresponding friction stress again after the follow-up shears, so as to approximately restore the corresponding peak shear strength of each shear of discontinuities.

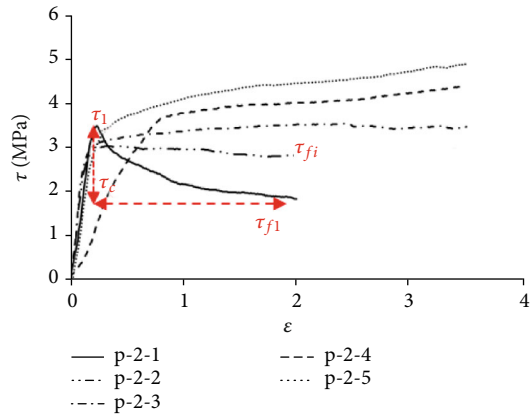

Figure 10: Diagram of strength components.

$$\tau_i = \tau_c + \tau_{fi}, \tag{7}$$

where $i = 2, 3, 4, 5$, which refers to the ith test.

Therefore, according to the above theory and combined with test results, the peak strength of each shear of discontinuities is restored approximately, as shown in Table 2.

After certain correction, each block of the discontinuities has a good linear correlation with the peak shear strength under different normal forces, so as to finally determine the basic mechanical parameters of the discontinuities, as shown in Table 3 and Figure 11.

5.2. Empirical Formula of Shear Strength Considering 3D Morphology. The peak shear strength of discontinuities has always been a hotspot and difficult subject in the field of rock mass mechanics in the past few decades. Most of the peak shear strength formulas proposed so far follow the form of the Mohr-Coulomb formula. Barton first proposed that the shear strength of discontinuities is mainly composed of three parts: peak dilation angle, i.e., the dip of shear path tangent in the peak state; convex shear part, which represents the contribution of convex shear damage to jointed strength; and basic friction angle, which is mainly determined by material properties [5]. Based on the direct shear test on irregular discontinuities in the state of normal stress, Patton considered that the irregular jointed surface morphology has a significant impact on the peak shear strength of the joint [35]. Therefore, Patton established a relational expression between dilation angle and normal stress with different morphological parameters, deeming that the shear strength of the joint is jointly determined by normal stress (σ_n) and internal friction angle (φ_b).

$$\tau_p = \sigma_n \tan\left(\varphi_b + i_p\right), \tag{8}$$

where τ_p refers to the peak shear strength, σ_n refers to the normal stress, φ_b refers to the internal friction angle, and i_p refers to the dilation angle.

Based on the Patton model and in combination with the model of Qian [36], the empirical formula for shear strength of discontinuities was proposed by considering the influence of 3D morphology:

$$\tau_p = \sigma_n \tan\left[\varphi_b + \arctan\left(Z_2\right)\right], \tag{9}$$

where τ_p refers to peak shear strength, σ_n refers to normal

Table 2: Peak shear strength of discontinuities (unit: MPa).

Sample No.	τ_1	τ_{f1}	τ_c	τ_2	τ_{f2}	τ_3	τ_{f3}	τ_4	τ_{f4}	τ_5	τ_{f5}
p-1	2.75	1.94	0.81	3.74	2.93	4.99	4.18	5.89	5.08	6.69	5.88
p-2	3.47	1.84	1.63	4.45	2.82	5.14	3.51	5.62	3.99	6.06	4.43
p-3	2.7	2.5	0.2	3.34	3.14	4.81	4.61	5.53	5.33	6.35	6.15
p-4	3.13	2.33	0.8	3.99	3.19	5.32	4.52	5.73	4.93	6.1	5.3
p-5	3.7	3.13	0.57	4.89	4.32	6.06	5.49	7.37	6.8	8.17	7.6

Table 3: Basic mechanical parameters of discontinuities.

Sample No.	2.5	3.25	5	6.25	7	Fitted curve	R^2	Frictional angle φ (°)	Cohesive force (c)
p-1	2.75	3.74	4.99	5.89	6.69	$y = 0.8269x + 0.843$	0.9913	39.61	0.843
p-2	3.47	4.45	5.14	5.62	6.06	$y = 0.52x + 2.4522$	0.9543	27.49	2.4522
p-3	2.7	3.34	4.81	5.53	6.35	$y = 0.788x + 0.7637$	0.9953	38.26	0.7637
p-4	3.13	3.99	5.32	5.73	6.1	$y = 0.6412x + 1.7764$	0.9643	32.68	1.7764
p-5	3.7	4.89	6.06	7.37	8.17	$y = 0.9392x + 1.5298$	0.9879	43.23	1.5298

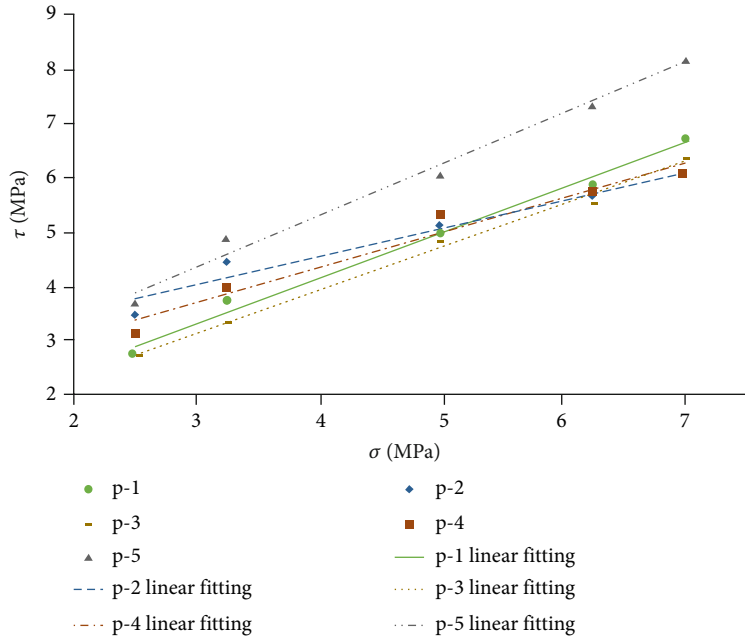

Figure 11: Relationship between different normal stresses and shear forces on discontinuities.

stress, and φ_b refers to internal friction angle. When the normal stress is 0, arctan (Z_2) can be used to characterize the initial dilation angle that is related to 3D morphological properties of the joint. As for smooth flat discontinuities, the 3D morphological parameter is 0, and the formula is simplified into $\tau_p = \sigma_n \tan(\varphi_b)$, which is consistent with the classical Mohr-Coulumb criterion.

The comparison between the test result of peak shear strength of discontinuities and the calculated result of the formula (9) is shown in Figure 12, from which it can be seen that the theoretical value of formula (9) and test result maintain good consistency at the beginning of the cycle. As the number of cycles increases, the deviation between test value and theoretical value grows, which is because the test value of peak shear strength has been restored by certain means, but as the normal pressure increases, the peak shear strength restored is still low, so that the deviation grows under high normal stress.

The empirical formula of shear strength considering 3D morphological parameters of discontinuities obtained is simple and clear in expression, each of whose parameters can be obtained quickly, and it can be used to rapidly evaluate the morphological properties and estimate the shear strength of discontinuities, so that it is suitable for the discontinuities of hard rock mass.

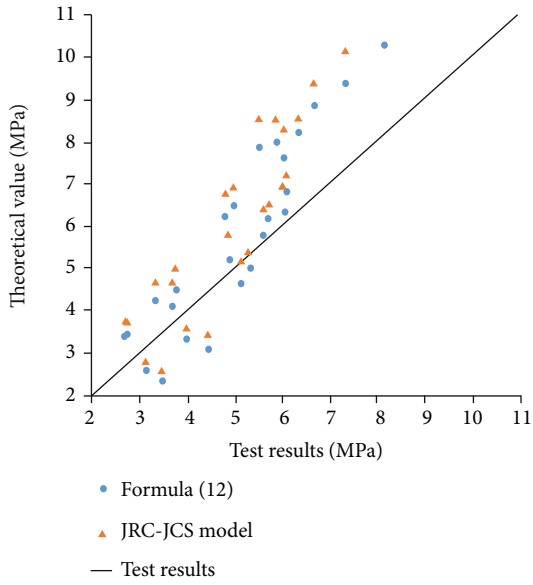

Figure 12: Comparison diagram of test results and theoretical value of the model.

5.3. Model Validation of Shear Strength considering 3D Morphology. Barton and Choubey [5] proposed the most commonly used JRC-JCS formula based on a large number of direct shear tests on the discontinuities of rock mass:

$$\tau = \sigma_n \times \tan\left[JRC \lg\left(\frac{JCS}{\sigma_n}\right) + \varphi_b\right], \tag{10}$$

where φ_b refers to the basic internal friction angle, σ_n refers to the normal stress, and JCS refers to the compressive strength of the wall of discontinuities.

Based on Barton's standard profile line, Tse and Cruden [29] found by studying surface geometrical parameters that the correlation between the root-mean-square (Z_2) of slope and roughness coefficient JRC of discontinuities is the best, and the correlation coefficient is 0.986, as shown in formula (12). In this paper, the root-mean-square (Z_2) is substituted into formula (11) in order to deduce the roughness coefficient JRC of discontinuities, which is later substituted into formula (10) in order to calculate the corresponding peak shear strength. The calculation results are shown in Figure 12.

$$JRC = 32.20 + 32.47 \lg(Z_2)\ [29]. \tag{11}$$

In order to quantitatively evaluate the effect of two models on the predicted peak shear strength, the mean deviation formula is used to characterize the accuracy of the calculation model, and the smaller the mean deviation is, the closer the calculated value of the model is to the measured value. The mean deviation is defined below [37–39]:

$$\bar{\sigma}_{avg} = \frac{1}{n}\sum_{i=1}^{n}\left|\frac{\tau_{mea} - \tau_{est}}{\tau_{mea}}\right| \times 100\%, \tag{12}$$

Table 4: Mean deviation between calculated value and test value of two models.

	After first shear	After first two shears	After three shears	After four shears	After five shears
Formula (11)	22.12%	21.23%	20.81%	21.48%	21.40%
JRC-JCS	27.40%	26.24%	25.39%	27.35%	27.63%

where $\bar{\sigma}_{avg}$ refers to mean deviation, τ_{mea} refers to the test value of jointed peak shear strength, τ_{est} refers to the calculated value of jointed peak shear strength, and n refers to the number of joint test groups.

Based on 25 shear tests, the mean deviations of formula (9) and JRC-JCS formula in different stages are shown in Table 4. If analyzed from mean deviation, it can be seen that as the number of cycles increases, the mean deviation of formula (9) remains stable and is smaller than that of the classical JRC-JCS formula, which indicates that the model has stable prediction ability, the calculated value can be well fitted with the test value, and the model effect is superior to the classical Barton's formula.

6. Conclusion

In this paper, an integrated study is carried out on the morphological properties and shear properties of the discontinuities of natural rock mass, and a high-accuracy 3D morphology scanning test on the discontinuities is conducted to evaluate the 3D morphological properties of the discontinuities of rock mass. In addition, based on the graded cyclic shear test of discontinuities, the impact of the morphological properties of discontinuities of natural rock mass on the strength properties and deformation properties of discontinuities are analyzed and concluded, and the main conclusions are as follows:

(1) Based on the results of the 3D morphology scanning test on the discontinuities of natural rock mass, the root-mean-square (Z_2) of slope is selected as the parameter for evaluating morphological properties, and it is found that the morphological parameter shows a trend of steady decline as the number of shears increases

(2) Based on the graded cyclic shear test curve, the graded cyclic shear properties of the discontinuities of rock mass are analyzed from shear deformation, and the shear process of discontinuities is refined in combination with the characteristics of the change in shear stiffness

(3) Based on the graded cyclic shear test on the discontinuities of natural rock mass, the strength properties and deformation properties of discontinuities in the process of graded cyclic shear process are analyzed, and a method that is suitable for determining the strength parameter of discontinuities in the graded

cyclic shear process is proposed. Also, combined with the 3D morphological parameter, the empirical formula of shear strength of discontinuities considering 3D morphological properties is proposed, which is compared with the classical JRC-JCS formula in order to validate the proposed shear strength model.

Data Availability

All data and models generated or used during the study appear in the submitted article.

Conflicts of Interest

The authors declare that they have no conflicts of interest.

Acknowledgments

This work was supported by the National Natural Science Foundation of China (No. 41977227), the Key Laboratory of Rock Mechanics and Geohazards of Zhejiang Province, Key Technology of Highway Tunnel Safety Construction Under Complex Condition in Eastern Yunnan Mountainous Area, Research on Key Technology of Corrugated Steel Assembly Rapid Initial Support Structure for Highway Tunnel, the Shanghai Rising-Star Program (No. 17QC1400600), and the Shanghai Municipal Science and Technology Major Project (No. 2017SHZDZX02).

References

[1] Q. Z. Zhang, *Study on the shear creep characteristics of rock mass discontinuity*, Tongji University, 2011.

[2] D. L. Qi, *Fuzzy measure method of the analysis for jointed rock slope stability*, Hebei University, 2015.

[3] Z. Y. Luo, S. G. Du, and M. Huang, "Experimental study of stress effect on peak friction angle of rock structural plane," *Chinese Journal of Rock Mechanics and Engineering*, vol. 33, no. 6, pp. 1142–1148, 2014.

[4] C. C. Xia and Z. Q. Sun, *Joint mechanics of engineering rock mass*, Tongji University Press, 2002.

[5] N. Barton and V. Choubey, "The shear strength of rock joints in theory and practice," *Rock Mechanics*, vol. 10, no. 1-2, pp. 1–54, 1977.

[6] Y. Li and Y. Zhang, "Quantitative estimation of joint roughness coefficient using statistical parameters," *International Journal of Rock Mechanics and Mining Sciences*, vol. 77, pp. 27–35, 2015.

[7] G. Zhang, M. Karakus, and H. Tang, "A new method estimating the 2D joint roughness coefficient for discontinuity surfaces in rock masses," *International Journal of Rock Mechanics and Mining Sciences*, vol. 72, pp. 191–198, 2014.

[8] X. G. Liu, W. C. Zhu, and Q. L. Yu, "Estimation of the joint roughness coefficient of rock joints by consideration of two-order asperity and its application in double-joint shear tests," *Engineering Geology*, vol. 220, pp. 243–255, 2017.

[9] S. G. Du, S. F. Yang, and Z. Jiang, "A new technique for fast measurement of," *Journal of Engineering Geology*, vol. 10, no. 1, pp. 98–102, 2002.

[10] B. B. Mandelbrot, "The fractal geometry of nature," *American Journal of Physics*, vol. 51, no. 3, pp. 286-287, 1983.

[11] P. H. S. W. Kulatilake, P. Balasingam, J. Park, and R. Morgan, "Natural rock joint roughness quantification through fractal techniques," *Geotechnical and Geological Engineering*, vol. 24, no. 5, pp. 1181–1202, 2006.

[12] Z. D. Zhu, F. D. Xing, and W. P. Qu, "Fractal description of two-phase medium cementation plane roughness coefficient between rock and concrete," *Journal of China Coal Society*, vol. 31, no. 1, pp. 20–25, 2006.

[13] T. Belem, F. Homand-Etienne, and M. Souley, "Quantitative parameters for rock joint surface roughness," *Rock Mechanics and Rock Engineering*, vol. 33, no. 4, pp. 217–242, 2000.

[14] G. Grasselli, J. Wirth, and P. Egger, "Quantitative three-dimensional description of a rough surface and parameter evolution with shearing," *International Journal of Rock Mechanics and Mining Sciences*, vol. 39, no. 6, pp. 789–800, 2002.

[15] C. C. Xia, W. M. Xiao, and W. Wi, "Calculation method for three-dimensional composite topography of joint under different contact conditions," *Chinese Journal of Rock Mechanics and Engineering*, vol. 29, no. 11, pp. 2203–2210, 2010.

[16] T. Rabczuk, G. Zi, S. Bordas, and H. Nguyen-Xuan, "A simple and robust three-dimensional cracking-particle method without enrichment," *Computer Methods in Applied Mechanics & Engineering*, vol. 199, no. 37-40, pp. 2437–2455, 2010.

[17] T. Rabczuk and T. Belytschko, "Cracking particles: a simplified meshfree method for arbitrary evolving cracks," *International Journal for Numerical Methods in Engineering*, vol. 61, no. 13, pp. 2316–2343, 2004.

[18] N. Barton, "Review of a new shear-strength criterion for rock joints," *Engineering Geol*, vol. 7, no. 4, pp. 287–332, 1973.

[19] S. G. Chen, J. G. Cai, and J. Zhao, "Discrete element modelling of an underground explosion in a jointed rock mass," *Geotechnical and Geological Engineering*, vol. 18, no. 2, pp. 59–78, 2000.

[20] J. W. Park, Y. K. Lee, and J. J. Song, "A constitutive model for shear behavior of rock joints based on three-dimensional quantification of joint roughness," *Rock Mechanics and Rock Engineering*, vol. 46, no. 6, pp. 1513–1537, 2013.

[21] C. C. Xia, Z. C. Tang, and Y. L. Song, "A new peak shear strength formula for matching irregular joints based on 3D morphology parameters," *Chinese Journal of Rock Mechanics and Engineering*, vol. 32, no. S1, pp. 2833–2839, 2013.

[22] Y. F. Ge, *Research on roughness and peak shear strength for rock discontinuities based on BAP*, China University of Geosciences, 2014.

[23] B. Laganyi and G. Archambault, "Simulation of shear behaviour of a jointed rock mass," *Proceedings of the 11th Symp. on Rock Mechanics. [S. l.]*, W. H. Somerton, Ed., , pp. 105–125, AIME, 1970.

[24] N. Barton, *Modeling rock joint behavior from in-situ block tests: implications for nuclear waste repository design*, Office of Nuclear Waste Isolation, Columbus, 1982.

[25] X. J. Yin, G. L. Wang, and C. H. Zhang, "Study of constitutive model for rock interfaces and joints under cyclic shear loading," *Engineering Mechanics*, vol. 22, no. 6, pp. 97–103, 2005.

[26] Q. S. Li and S. J. Du, "Surface roughness analysis of rock joints under different shear deformation histories," *Rock and Soil Mechanics*, vol. 6, pp. 850–855, 2004.

[27] D. Huang, R. Q. Huang, and L. Pe, "Shear deformation and strength of through-going saw-tooth rock discontinuity," *Journal of China Coal Society*, vol. 7, 2014.

[28] Y. Gui, *Study on the surface degradation under shearing and the coupled shear-flow properties of rock joints*, Tongji University, 2018.

[29] R. Tse and D. M. Cruden, "Estimating joint roughness coefficients," *International Journal of Rock Mechanics & Mining Sciences & Geomechanics Abstracts*, vol. 16, no. 5, pp. 303–307, 1979.

[30] X. B. Yu and B. Vayssade, "Joint profiles and their roughness parameters," *International. Journal of Rock Mechanics and Mining Sciences*, vol. 28, no. 4, pp. 333–336, 1991.

[31] B. S. A. Tatone and G. Grasselli, "A new 2D discontinuity roughness parameter and its correlation with JRC," *International Journal of Rock Mechanics and Mining Sciences*, vol. 47, no. 8, pp. 1391–1400, 2010.

[32] B. Ladanyi and G. Archambault, "Simulation of shear behavior of a jointed rock mass," in *The 11th US Symposium on Rock Mechanics. American Rock Mechanics Association*, OnePetro, 1969.

[33] Z. Wang, M. R. Shen, G. H. Tian, and Q. Z. Zhang, "Time-dependent strength of rock mass discontinuity with different values of JRC," *Chinese Journal of Rock Mechanics and Engineering*, vol. 36, Supplement 1, pp. 3287–3296, 2017.

[34] Z. Wang, L. L. Gu, M. R. Shen, F. Zhang, G. K. Zhang, and S. X. Deng, "Influence of shear rate on the shear strength of discontinuities with different joint roughness coefficients," *Geotechnical Testing Journal*, vol. 43, no. 3, p. 20180291, 2020.

[35] F. D. Patton, "Multiple modes of shear failure in rock," in *In Proc First Congress of International Society of Rock Mechanics*, pp. 509–513, Lisbon, Portugal, 1966.

[36] X. Qian, *Study of shear-flow coupled behaviors of rock joints under high seepage pressure*, Tongji University, Changsha, 2018.

[37] P. H. S. W. Kulatilak, G. Shou, and T. H. Huang, "New peak shear strength criteria for anisotropic rock joints," *International Journal of Rock Mechanics & Mining Sciences & Geomechanics Abstracts*, vol. 32, no. 7, pp. 673–697, 1995.

[38] J. Yang, G. Rong, and D. Hou, "Experimental study on peak shear strength criterion for rock joints," *Rock Mechanics and Rock Engineering*, vol. 49, no. 3, pp. 821–835, 2016.

[39] N. Vu-Bac, T. Lahmer, X. Zhuang, T. Nguyen-Thoi, and T. Rabczuk, "A software framework for probabilistic sensitivity analysis for computationally expensive models," *Advances in Engineering Software*, vol. 100, pp. 19–31, 2016.